Contrast of Coronal Holes and Parameters of Quiet Solar Wind

Obridko V.N.[1], Shelting B.D.[1], Asgarov A.B.[2].

(1) Pushkov Institute of Terrestrial Magnetism, Ionosphere, and Radio Wave Propagation (IZMIRAN), Russian Academy of Sciences

(2) Shemakha Astrophysical Observatory (ShAO), National Academy of Sciences of Azerbaijan Republic

It is shown that the contrast of coronal holes, just as their size, determines the velocity of the solar wind streams. More than 500 measurements in λ 284 A have been analyzed. The time interval under examination covers about 1500 days in the declining phase of cycle 23. All coronal holes recorded for this interval in the absence of coronal mass ejections have been studied. The comparison with some other parameters (e.g. density, temperature, magnetic field) was carried out. The correlations are rather high (0.70-0.89), especially during the periods of moderate activity, and could be used for everyday forecast. The contrast of coronal holes is rather small. On the average, it is 0.08 of the ambient solar atmosphere, ranging from 0.04 to 0.013.

1. Introduction. Statement of the Problem

Shortly after the discovery of coronal holes (CH) in the Sun, it became clear that they were associated with high-speed streams (HSS) of the solar wind (SW). Nolte et al. (1976) established a close relationship between the CH area and the speed to the solar wind outflow from the latter. CH are sources of fast solar wind (Gosling and Pizzo, 1999, Zhang et al., 2002, 2003; McComas and Elliott, 2002, Bromage, Browning, and Clegg, 2001), forming high-speed streams near the Earth.

Coronal holes (CHs), are mainly observed in X-rays, extreme ultraviolet, and radio wavelengths appear as dark regions (Bromage, Browning, and Clegg, 2001; Chertok et al., 2001, Kahler and Hudson, 2002) in the images.

There are also physical reasons to believe that the brightness (contrast) of CH must correlate with some characteristics of the associated high-speed solar wind, first of all, with its velocity. This suggestion was made about ten years ago in (Obridko, 1998; Obridko et al., 2000) and has not been verified ever since. Another relationship, i.e., the correlation between the velocity and CH area, has been verified repeatedly (Veselovsky et al., 2006; Robbins et al., 2006, Vrsnak et al., 2007a, b). In particular, Robbins et al. (2006) have shown that the correlation between the solar wind velocity and CH area decreases in the epochs of high solar activity. This should be expected, because coronal mass ejections (CME) not related directly to coronal holes produce sudden bursts of speed that upset the correlation with the CH area. Besides, the role of the closed field lines responsible for the particularly slow solar wind streams increases in the periods of high solar activity. Vrsnak et al. (2007a, b) studied the relationship between the solar wind velocity and CH area in a relatively quiet period – from January to May, 2005, and obtained a reasonably high correlation coefficient (0.62) at a transport time of 4 days.

The relationship between the magnetic field in the coronal hole and the solar wind velocity was analyzed by many authors. Thus, Obridko et al, (2004,2006), Belov et al. (2006) obtained quite a high correlation between the magnetic field parameters in the Sun and the speed of the solar wind. Predictions of the solar wind speed at the Earth are regularly made by several groups based on solar potential field extrapolations. This set of forecasts is based on extrapolation of photospheric longitudinal magnetic field measurements using a potential field assumption to locate open field lines. Using one of these models, a modified Wang and Sheeley (1990, 1992) flux-transport model, Arge and Pizzo (2000) studied a three-year period centered about the May 1996 solar minimum. They compared the predicted solar wind speed and magnetic polarity with observations near the Earth. Their three-year sample period had an

overall correlation of ~ 0.4 with the observed solar wind velocities. Later on, the model was updated significantly. In this model, the SW velocity at the Earth orbit depends on the local expansion of the magnetic field calculated under potential approximation (Arge et al. 2003, 2004). The results of the regular forecast of SW velocity by this method are available on the Internet site http://solar.sec.noaa.gov/ws/.

However, since the CH brightness (contrast) depends on the divergence of the field lines, which also determines the HSS velocity (Wang-Sheeley parameter), the correlation between the CH contrast and HSS velocity is physically expected, and it should be a reasonable parameter for geophysical forecast.

Today it is fairly clear that these zones are dominated by open magnetic field lines. They act as efficient conduits for flushing heated plasma from the corona into the solar wind. Because of this efficient transport mechanism, coronal holes are empty of plasma most of the time and thus appear much darker than the other places of the Sun.

This coarse temperature characterization of the corona already shows an interesting trend. Open-field regions, such as coronal holes, have the coolest temperatures of T ~ 1 MK; closed-field regions, such as the quiet Sun, have intermediate temperatures of T~ 2 MK; while active regions exhibit the hottest temperatures of T~ 2-6 MK. Open-field regions seem to be cooler because plasma transport is very efficient, while closed-field regions seem to be hotter because the heated plasma is trapped and cannot easily flow away. The temperature difference between quiet Sun and active regions is a consequence of different magnetic emergence rates, heating rates, conductive loss rates, radiative loss rates, and solar wind loss rates (Cushman and Rense, 1976; Rottman, Orrall, and Klimchuk, 1982; Orrall, Rottman, and Klimchuk, 1983; Cranmer, 2002a, 2002b.).

It is still unknown to what extent the solar wind is fed by flux tubes that remain open (and are energized by footpoint driven wavelike fluctuations), and to what extent much of the mass and energy is input more intermittently from closed loops into the open-field regions. It is notable that both the WTD and RLO models have recently passed some basic "tests" of comparison with observations. Both kinds of model have been shown to be able to produce fast (v~700 km/s), low-density wind from coronal holes and slow (v ~ 400 km/s), high-density wind from streamers rooted in quiet regions. Both kinds of model also seem able to reproduce the observed *in situ* trends of how frozen-in charge states and the FIP effect vary between fast and slow wind streams. Note here that, unlike the regular corona where the heat conduction loss is dominating, the loss in the coronal holes is mainly through the solar wind outflow (Withbroe and Noyes, 1977). Thus, the very fact of darkening in the coronal holes is, undoubtedly, associated with the outgoing high-speed streams. This conclusion was drawn in (Badalyan and Obridko, 2004, 2007).

Many uncertainties that will be discussed below have prevented us so far from using directly the hypothesis of correlation between the CH brightness and solar wind velocity proposed in our earlier work (Obridko, 1998; Obridko et al., 2000). The brightness ("darkness") of coronal holes was used as a subsidiary qualitative prognostic factor at the Center of Forecasts of IZMIRAN. However, it was difficult to verify this correlation and obtain quantitative characteristics.

The advantage of this method in comparison with the method by Wang-Sheeley-Arge based on the magnetic field model is that we establish a correspondence between two directly observed events without any additional theoretical assumptions.

Lately, in (Luo et al, 2008), the CH brightness in the line 284 A was used to calculate the solar wind velocity at the Earth, and rather a high correlation was obtained during a relatively short time interval from November 21 to December 26, 2003. It should be noted, however, that the authors did not use as a prognostic index the CH brightness as such, but rather the inverse brightness in each pixel averaged over a fixed circle at the center of the Sun. This value may differ significantly from the mean brightness. Its physical interpretation is not an easy matter, since in all mechanisms of heating and energy transport we are dealing with the brightness rather

than its inverse value. Besides, averaging all inverse brightness values inside a fixed circle may involve nonstationary processes, such as flares and coronal mass ejections, and thus, corrupt the index obtained.

Therefore, we have chosen to use the pixel brightness directly and to investigate the potential sources of uncertainty associated both with the physical analysis of CH brightness and with its prognostic application. Check calculations have been performed for several periods, including those analyzed in (Vrsnak, Temmer, and Veronig, 2007a,b) and (Luo et al, 2008).

2. Uncertainties in the Problem Solution

The difficulties are due to the fact that many characteristics and even terms are poorly defined. Unfortunately, no quantitative criteria have been used until now to precisely locate CH from observations (Zhao, Hoeksema, and Scherrer, 1999).

In particular, it is not clear where the CH boundary passes, what wavelengths it should be studied at, how it can be discriminated from the filament-type features, how the contrast is determined, what is the undisturbed region, and how the potential degradation of receivers can be allowed for. We do not know whether the polar and equatorial holes must be analyzed separately.

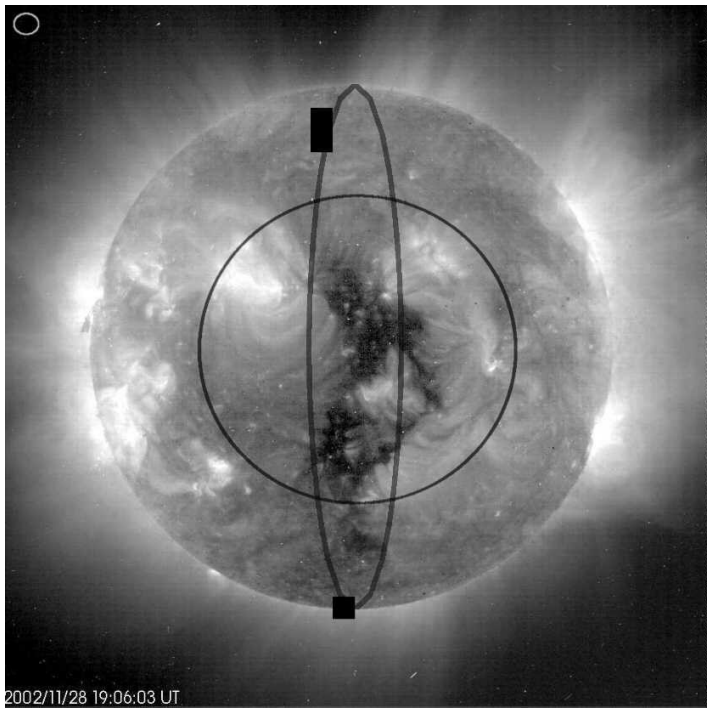

Fig. 1. The coronal hole observed in the line λ284 A on November 28, 2002. The fog measuring site on this image is marked with a circle in the upper left corner (see 2.2). The boundaries of the spherical sector and the circle of radius 0.6 R_0.are indicated.

Fig. 1 illustrates the situation on the disk as observed on November 28, 2002 in the line λ284 A. One can see a complex feature of CH type with multiconnected contours, whose boundaries are extremely difficult to identify. Since the inner structure of the hole is highly inhomogeneous, it is not clear whether we should find the minimum brightness, mean brightness, or complete integral deficit of brightness (speaking metaphorically, the "maximum depth, mean depth, or volume of the canyon"). Correlation with the solar wind parameters involves additional difficulties associated with identifying the CH effect and eliminating the other processes, first of all, coronal mass ejections. Therefore, the problem is solved by stages.

The contrast is determined by the method commonly used in the photometry of the spectral lines or sunspot contrast. We need for calculation the measurements of the background

or fogging (in our case, outside of the disk), brightness in CH, and variation of undisturbed region (equivalent of the continuum in the spectral photometry). Even so, it is not clear if the deficit should be referred to the mean brightness of the disk, which contains many isolated, very bright features, or to the CH immediate environment.

Note also that, though coronal holes are sharply outlined on the photo, their real qualitative contrast is very small compared to sunspots.

There is also another problem to be solved. We may compare the CH brightness and solar wind velocity only on the days of real passage of CH over the disk. Alternatively, we may simulate the everyday forecast by calculating the prognostic indices for each day no matter whether any CH were observed or not. In doing so, we must, naturally, exclude the days when coronal mass ejections were recorded.

Correlation with the solar wind parameters involves one more source of uncertainty, i.e., the transport time. Note that the optimal transport time may not be the same for different parameters.

2.1. PROVISIONAL REVIEW OF DATA

In the epochs of solar maximum, the polar holes are absent; however, the number of the equatorial holes, which are best suited for correlation with the solar wind parameters, increases. On the other hand, these are the periods when undisturbed regions are scarce, and there is a high probability that the velocity increase is associated with CME rather than CH.

In the epochs of minimum, on the contrary, the equatorial holes are virtually not observed, while the polar ones are ever present. Undisturbed zones are easier to isolate than in the epochs of maximum. Therefore, one can simply use daily measurements to calculate the total daily area of the regions in the Sun below a certain limit.

To begin with, we have considered the following data for 1999: SOHO images at 171 A ($T\sim1.3\times10^4$K), 195 A ($T\sim1.6\times10^6$K), 284 A ($T\sim2.0\times10^6$K), and 304 A ($T\sim8.0\times10^4$K); Yohkoh X-ray images; sketches of CH observed at 10830 A from SGD; open magnetic fields calculated from Stanford observations using an original program, and a composite file of solar wind velocities at the Earth orbit. Four coronal holes were selected, whose passage through the central meridian could be connected more or less reliably with the increase of SW velocity.

The optimal line for the problem under consideration turned out to be 284 A.

The contrast is determined by the method commonly used in photometry of the spectral lines or sunspot contrast. We need for calculation the measurements of the background or fogging. A review of the data for 2005 has shown that the fog does not virtually change during the year and is determined with an error less than 0,2%.

The brightness of undisturbed region is extremely uncertain and, therefore, can hardly be used.

As the conventional CH boundary or (what is the same in our case) the brightness of the undisturbed CH environment, we have taken 1.03 of the background value. As shown by preliminary estimates, this does not affect much the result, because the boundary brightness in coronal holes changes rapidly. The indices obtained alter a little if we use the values of 1.035 and 1.04 of the background brightness, but the correlation with the solar wind parameters remains virtually unchanged.

The calculations for each day were performed for the whole disk, for a spherical sector ±1 day from the central meridian, and for a circle of radius equal to 0.6 solar radii. The boundaries of the spherical sector and the circle of radius 0.6 R_0.are marked in Fig. 1.

We did not introduce correction for the projection, and all areas were calculated as the number of pixels.

The defects like those seen in Fig. 1 were dealt with by taking the mean disk value for the pixels involved. This did not virtually affect the mean contrast.

2.2. THE DATA USED AND INDICES CALCULATED

Hereinafter, we have used SOHO data in fits-format 1024x1024 from the Internet *(*http://sohowww.nascom.nasa.gov/cgi-bin/summary_query_form*)*.

The list of coronal holes was taken from the site Coronal hole history (since late October 2002) - http://www.dxlc.com/solar/coronal_holes.html

Correlation was analyzed with the daily mean velocity V, magnetic field B, density n, and temperature T at the transport time equal to 2, 3, and 4 days. These data were downloaded from the Internet site http://nsssdc.gsfc.nasa.gov/omniweb/

The following characteristics were calculated for each day.

General characteristics

fog – the minimum brightness outside of the solar disk on the image
S1 – the total brightness of all pixels over the disk
d1 – the total number of pixels on the disk
ss1 – the mean brightness of a pixel on the disk **(ss1=s1/d1)**

Central characteristics calculated

a) ***inside a spherical sector of ±1 day from the central meridian or***
b) ***inside a circle of radius 0.6 R_0***

S2 – the total brightness of pixels
d2 – the number of pixels
ss2 – the mean brightness **(ss2=s2/d2)**

Characteristics of coronal holes calculated

a) inside a spherical sector of ±1 day from the central meridian or
b) inside a circle of radius 0.6 R_0

sk – the total brightness of the pixels that satisfy the "brightness less than **fi*fog**» condition. The value **fi** determining the CH boundary brightness was assumed to be equal to **1.03;**
dkd – the number of the pixels that satisfy the "brightness less than **fi*fog**» condition;
skd – the mean brightness of the pixels that satisfy the "brightness less than **fi*fog**» condition;
ou – the minimum brightness among the points assigned to the coronal hole.

Indices

cn1=(ss-skd)*dkd – the canyon volume provided that the undisturbed brightness equals the disk mean brightness;
A=dkd/d2 – the relative CH area inside the central sector. Corresponds to the index used in (Vrsnak, Temmer, and Veronig, 2007a,b);
cn2=(ss2-skd)*dkd – the canyon volume provided that the undisturbed brightness equals the mean brightness inside the central sector;
cn3=(1.03*fog-skd)*dkd – the canyon volume provided that the undisturbed brightness is **1.03*fog;**
dcn=1.03*fog-skd – the mean canyon depth provided that the undisturbed brightness is **1.03*fog;**
dmax=1.03*fog-ou – the maximum canyon depth provided that the undisturbed brightness is **1.03*fog.**

Some of these indices are indicated by way of example on the one-dimensional central profile of the disk for November 28, 2002 (Fig. 2).

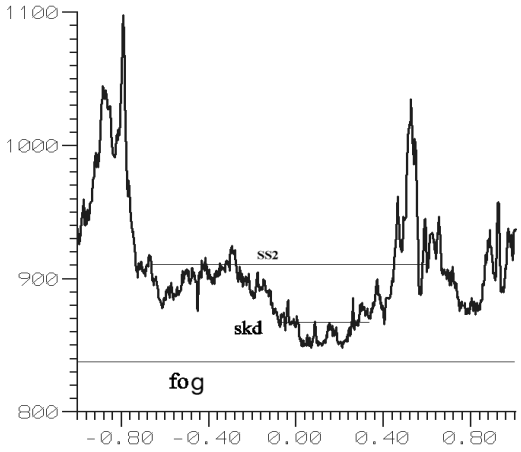

Fig. 2. One-dimensional central profile of the disk for November 28, 2002 with some indices marked.

The magnitudes R_0, X_0, and Y_0, which define the radius and coordinates of the disk center in pixels on the day under discussion, were taken from the file HEADER. This allowed us to take into account the eccentricity of the Earth orbit. The pixel size in seconds and the exposure, including the shutter release time, were also noted. However, the variation of the latter being negligible (<0.5%), no correction was introduced.

2.3. POSSIBILITY OF THE RECEIVER DEGRADATION

Represented in Fig. 3 are the mean brightness of the solar disk SS1 per pixel (squares, at the top) and the background brightness **fog** (circles, at the bottom). The abscissa shows the days beginning with January 1, 2002. One can see that both SS1 and **fog** decrease with time; however, the former decreases stronger than the latter. As a matter of fact, there is nothing to be surprised at, since the indices under discussion characterize different processes. **fog** accounts for the dark signal, which may change with time. The time variation of SS1 may indicate directly to the change of sensitivity of the receivers. Of course, it may also imply that the mean brightness of the Sun at the wavelengths of 284A decreases with the approach to the solar minimum.

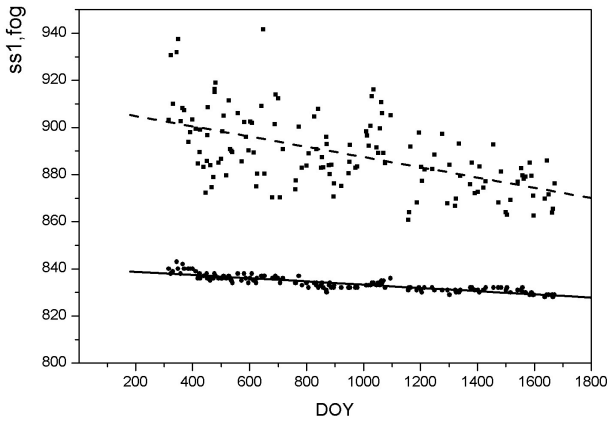

*Fig. 3. Mean brightness of the solar disk SS1 per pixel (squares, at the top) and the background brightness **fog** (circles, at the bottom).*

However, Fig. 4 reveals the relationship between the mean brightness of the solar disk per pixel SS1 and **skd,** i.e. the mean brightness of the pixels inside a circle of radius 0.6 R_0 that satisfy the "brightness less than **fi*fog**» condition. The observed high positive correlation

between these magnitudes is difficult to explain without suggesting a degradation of the receivers.

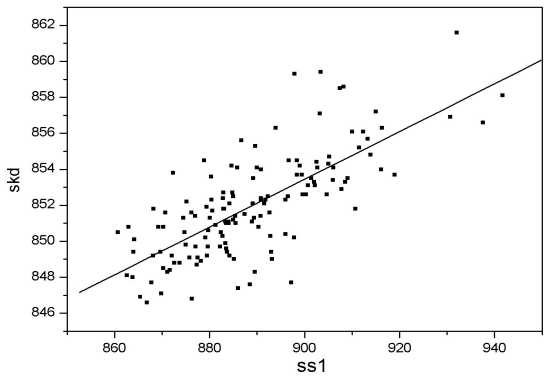

*Fig. 4. Relationship between the mean brightness of the solar disk per pixel **SS1** and **skd,** i.e. the mean brightness of the pixels inside a circle of radius 0.6 R_0 that satisfy the "brightness less than **fi*fog**» condition.*

As the first approximation to correction of this effect, we have plotted **dcn/(fi*fog)** vs. **SS1** (see Fig. 5). One can see that there is no significant correlation. On the whole, within the spread of the solar and SW data, a weak degradation of the receivers does not affect the correlation.

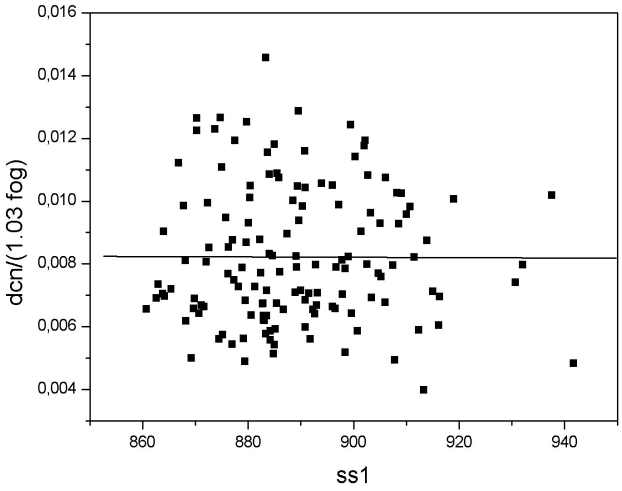

*Fig. 5. Mean relative contrast of coronal holes **dcn/(fi*fog)** compared to the mean brightness of the solar disk per pixel SS1.*

As noted above, the contrast of coronal holes is rather small. On the average, it amounts to 0.08 of the ambient regions ranging from 0.04 to 0.013.

2.4. TIME VARIATION OF CH PARAMETERS

Before turning to the study of correlation between the parameters of coronal holes and solar wind, let us consider their time variations. Fig. 6 represents the time variation of the relative area of coronal holes inside the central circle of radius 0.6 R_0. The abscissa shows the day numbers beginning with January 1, 2002. One can see that the relative area increases slightly with time even if the increase is not too reliable statistically.

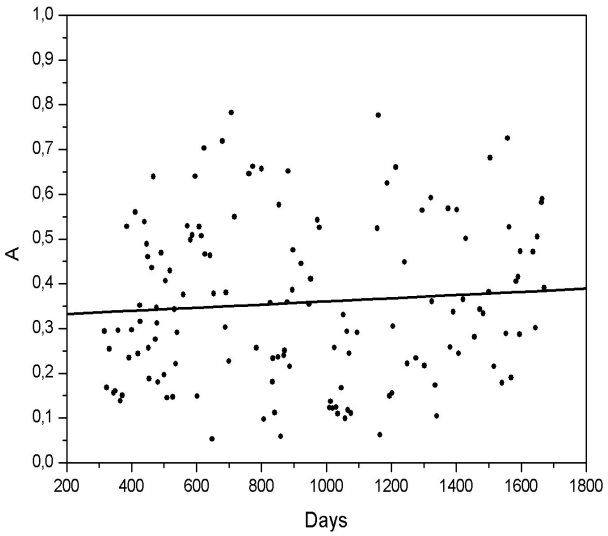

Fig. 6. Time variation of the relative area of coronal holes inside the central circle of radius 0.6 R_0

The very fact that the relative CH area does not decrease while approaching the solar minimum is surprising. It is well known that, at the minimum of the cycle, the equatorial coronal holes vanish, and the major, simply connected polar holes appear. This phenomenon has been discussed by various authors. Obridko and Shelting (1999) analyzed the evolution of open magnetic fields for the period 1970-1996 (Carrington rotations 1550-1915). The distribution of open field regions (OFR) over the solar disk changes sharply with the phase of the solar cycle. At the minimum, one can see simply connected regions at the poles. At the maximum, the distribution takes the form of small, isolated strips and cells. The change from one distribution pattern to another occurs over relatively short time intervals. At the end of the solar minimum, when the activity begins to increase, narrow streams and patches of open field emerge from the simply connected polar OFR and stretch to the equator. The polar region breaks down, but still exists up to the beginning of the maximum epoch, after which it vanishes rapidly. Then, during the whole phase of maximum, the open field regions have the form of narrow streams or crooked paths.

Fig. 7 illustrates the OFR evolution in cycle 23 for the period 1997-2007 (CR 1920-2060). This figure is obtained by the same method as was used to plot figure 1 in (Obridko and Shelting, 1999) and is a continuation of the latter.

It is seen that the equatorial open magnetic fields behave oddly enough at the minimum of cycle 23. Although we are having a prolonged sunspot minimum, the behaviour of the equatorial OFR is rather typical of the rise phase. This is, probably, why the tilt of the heliospheric current sheet has not reached its usual minimum values (see (Obridko and Shelting, 2009)).

On the other hand, the CH contrast, obviously, decreases as we approach the minimum. Fig. 8 demonstrates the time dependence of the mean (**dcn)** and maximum (**dmax)** deficit. This decrease (25% for **dcn** and 35% for **dmax)** is reliably identified and cannot be associated with the much weaker effect of degradation of the receivers. Probably, it manifests an increased fragmentation and diffusivity of CH in the vicinity of the solar minimum.

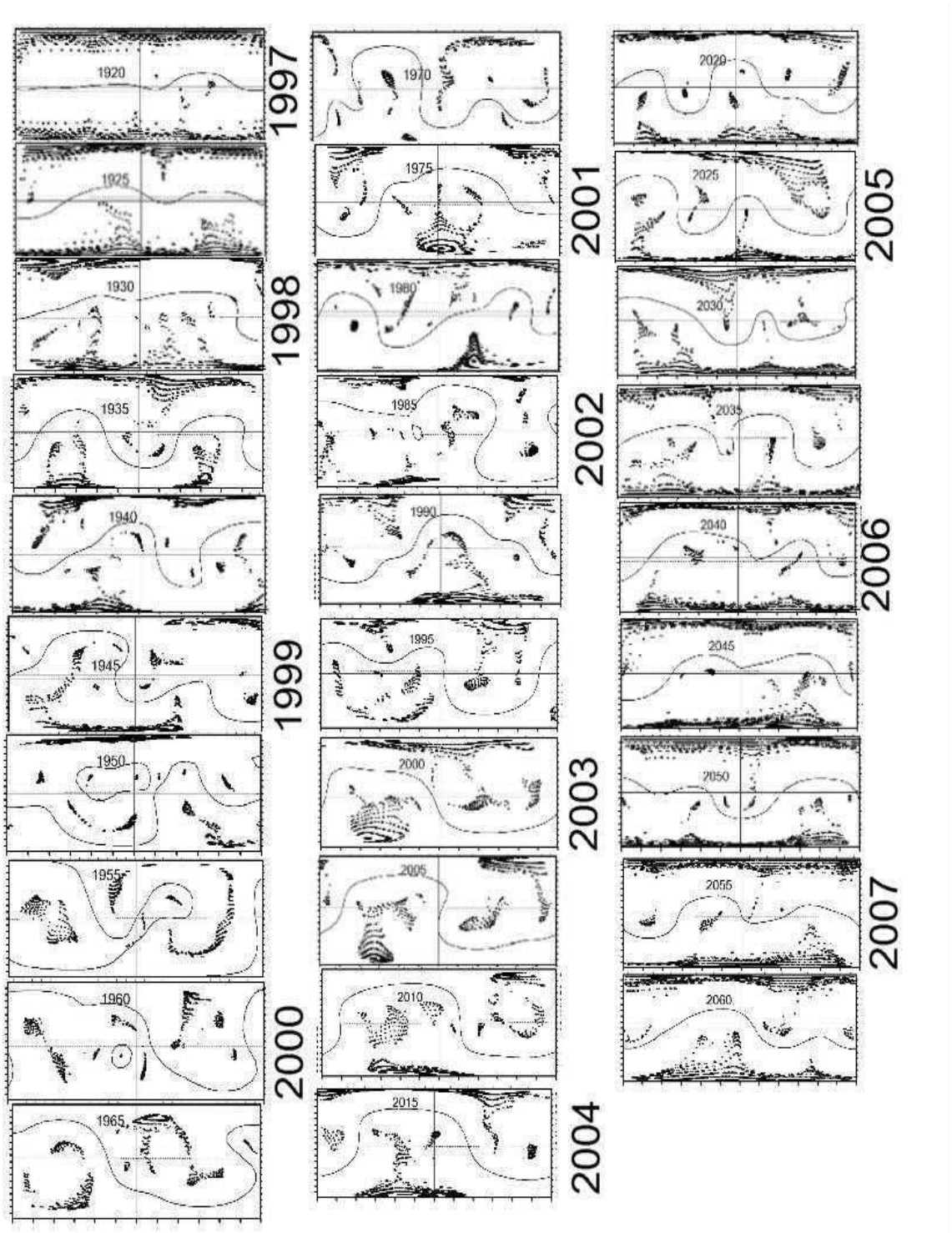

Fig. 7.Evolution of the Open Field Regions in cycle 23 for the period 1997-2007 (CR 1920-2060).

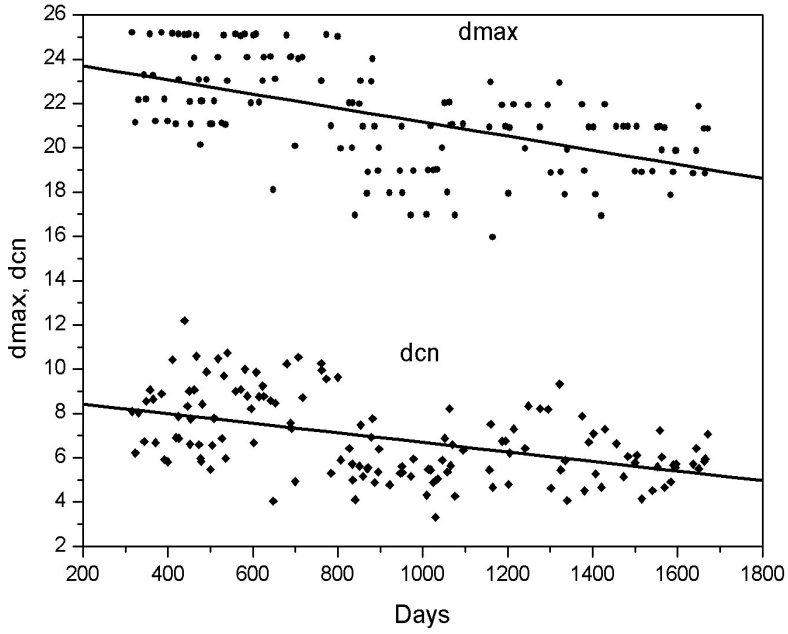

*Fig. 8. Time dependence of the mean (**dcn**) and maximum (**dmax**) deficit.*

3. CH Contrast and Solar Wind Characteristics

139 coronal holes for the period 2002-2006 have been selected from the file Coronal hole history (since late October 2002), i.e., all cases when the increase of the solar wind velocity at the Earth orbit was not associated with CME. Table 1 below provides the correlation between the solar wind parameters and CH brightness in the central sector. In this and other tables, the correlation coefficients higher than 0.5 are set off in bold type, and the cells with the correlation coefficient above 0.6 are shaded.

The comparison of five CH indices and four solar wind parameters infers that:

1. The index most appropriate for velocity calculations at a transport time of 4 days is the mean deficit ***dcn***.

2. The parameters under discussion are not as good as expected for the field and density calculations. We can only note that all of them display negative correlation with density on the fourth day, when the velocity is the greatest.

3. A fairly good positive correlation between the mean deficit ***dcn*** and temperature is obtained if we use a 2- or 3-day shift.

4. Calculating the magnetic field from CH brightness does not seem reasonable. The traditional methods of calculating the source-surface field from magnetographic data are more promising. In particular, such a technique was applied in (Belov et al., 2006).

In order to reveal the effect of polar coronal holes and take into account the chosen distance from the central meridian, we calculated all indices mentioned above inside a circle of radius 0.6 R_0 for the same 139 coronal holes. The results are tabulated below (Table 2).

TABLE 1

Correlation between the CH indices in the central sector and solar wind parameters

	Δt=2				Δt=3			
	B	V	n	T	B	V	n	T
A	0.28	0.35	0.05	0.40	0.00	0.48	-0.20	0.37
cn2	0.16	0.33	-0.05	0.33	0.21	0.30	-0.14	0.22
cn3	0.22	0.41	-0.05	0.42	0.00	0.49	-0.22	0.35
dcn	0.36	0.49	-0.06	**0.50**	0.24	**0.62**	-0.29	**0.51**
dmax	0.24	0.44	-0.10-	0.40	0.25	0.47	-0.23	0.39

	Δt=4			
	B	V	n	T
A	0.25	0.48	-0.33	0.22
cn2	0.12	0.26	-0.17	0.13
cn3	0.18	0.47	-0.29	0.22
dcn	0.00	**0.63**	-0.30	0.37
dmax	0.05	**0.51**	-0.28	0.36

TABLE 2

Correlation between CH indices within the central circle and solar wind parameters

	Δt=2				Δt=3			
	B	V	n	T	B	V	n	T
A	0.29	0.43	0.00	0.52	0.00	0.54	-0.23	0.41
cn2	0.26	0.25	-0.12	0.33	0.20	0.28	-0.11	0.24
cn3	0.32	**0.59**	-0.13	**0.63**	0.00	**0.65**	-0.32	0.48
dcn	0.36	**0.62**	-0.16	**0.60**	0.24	**0.67**	-0.33	**0.54**
dmax	0.23	0.53	-0.18	0.45	0.23	0.51	-0.26	0.40

	Δt=4			
	B	V	n	T
A	0.26	**0.54**	-0.36	0.30
cn2	0.10	0.30	-0.24	0.20
cn3	0.18	**0.65**	-0.39	0.40
dcn	0.00	**0.68**	-0.37	0.42
dmax	0.00	**0.53**	-0.35	0.39

Comparison of Tables 1 and 2 shows that, in the second one, the correlation between the indices under examination and the solar wind velocity has somewhat increased with allowance for the transport time Δt=3-4 days. To tell the truth, this increase exceeds but a little the correlation coefficient calculation error, which equals 0.04. However, the second method is more suitable for comparing the coronal holes observed on the disk with the solar wind velocity.

4. Calculation of Solar Wind Parameters in Everyday Forecast

At first sight, this problem is similar to direct correlation of the CH brightness deficit and solar wind characteristics. However, there are two items that make the situation somewhat different.

1. The everyday forecast involves the days when no coronal holes are observed on the Sun. This means that the total dynamic range of data is expanded.

2. On some days, coronal mass ejections are observed on the disk alongside with coronal holes, changing the velocity range dramatically. As seen below, the correlation between the brightness and solar wind velocity of such days breaks down completely.

4.1. CORRELATION ANALYSIS IN THE ABSENCE OF CME

First, we have analyzed the time interval from January 20 to June 5, 2005 (days of the year DOY 20-125), except for DOY 70-90, when no 284 A data were available. Since the halo CME were absent in that period, we can assume that solar wind was undisturbed, and its parameters were controlled solely by CH. The first part of the interval under examination coincides with that analyzed in (Vrsnak, Temmer, and Veronig, 2007a,b).

Tables 3 and 4 present the correlation of the calculated indices with B, V, n, T, and Ap at different transport times in the everyday forecast. As above, Table 3 refers to the spherical sector of ±1 day from the central meridian and Table 4, to the circle of radius 0.6 R_0.

Parameter ***dcn*** is, obviously, the best one. The highest correlation with V is observed on the fourth day; with B, on the second day; and with T, on the third day.

There are certain differences between Tables 1-2 and 3-4.

1.While the correlation between CH and solar wind parameters is higher in the circle of radius 0.6 R_0 (~3 days or ~37°. from the central meridian in the equatorial zone, the polar zones being excluded), the everyday forecast yields somewhat higher correlation coefficients when calculated in the spherical sector of ±1 day from the central meridian.

2.In the first case, negative correlation with ***n*** takes place at all transport times, while in the second one, it is only observed at 4-day shift.

3.A fairly good correlation with ***T*** has been revealed at Δt=3

4.Correlation with the geomagnetic index A_p is not high in all cases. To calculate this index correctly, we have to use data on the solar magnetic field (Belov et al., 2006).

TABLE 3

Correlation between the daily brightness deficit in the central sector and the solar wind parameters

	Δt=2					Δt=3				
	B	V	n	T	A_p	B	V	n	T	A_p
A	.29	.16	.27	.30	.28	.25	.49	.07	.46	.31
cn2	.48	.04	.27	.22	.16	.31	.18	.04	.35	.17
cn3	.37	.04	.33	.31	.33	.32	**.52**	.07	**.53**	.39
dcn	**.59**	.05	**.51**	.22	0.0	**.53**	.47	.14	**.63**	**.54**
dmax	.47	.0	.41	.17	0.0	.46	.44	.11	**.54**	.40

	Δt=4				
	B	V	N	T	A_p
A	.04	**.67**	-.19	**.51**	.32
cn2	.14	.26	-.13	.24	.13
cn3	.05	**.71**	-.24	**.52**	.33
dcn	.32	**.74**	-.21	**.55**	.37
dmax	.24	**.66**	-.21	**.54**	.31

TABLE 4

Correlation between the daily brightness deficit in the central circle and the solar wind parameters

	Δt=2				Δt=3			
	B	V	n	T	B	V	n	T
A	.27	.17	.26	.29	.23	.47	.00	.45
cn2	.39	.12	.18	.36	.24	.24	-.08-	.33
cn3	.36	.14	.32	.31	.31	**.50**	.03	**.50**
dcn	**.59**	.03	.49	.27	**.55**	.48	.10	**.60**
dmax	.45	.10	.36	.28	.37	.45	.29	**.51**

	Δt=4			
	B	V	N	T
A	.00	**.62**	-.20	.47
cn2	.06	.22	-.26	.24
cn3	.06	**.68**	-.24	**.50**
dcn	.26	**.68**	-.30	.49
dmax	.04	**.63**	-.28	**.52**

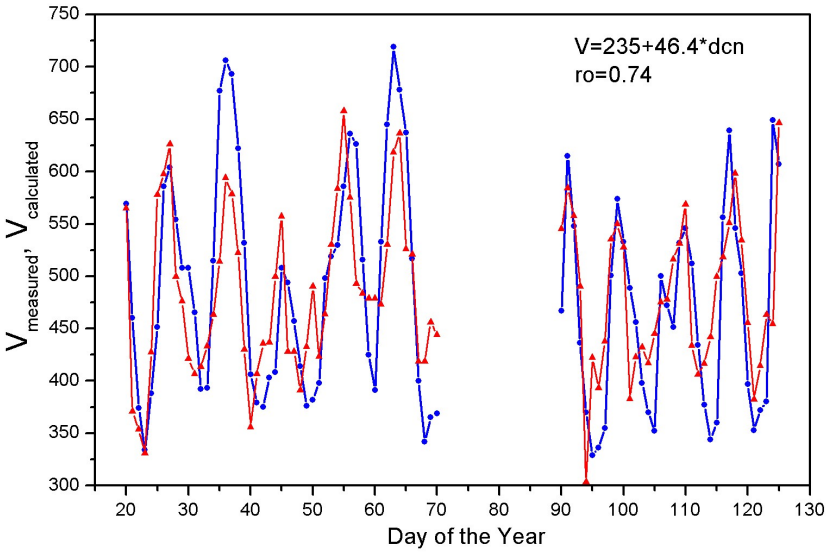

Fig. 9. Solar wind velocity measured (blue) and calculated (red) during the time interval from January 20 to July 2005. The abscissa shows the observation time in the Sun; the solar wind data are given with a shift of 4 days.

Fig. 9 represents the solar wind velocity both measured (blue) and calculated using the regression equation **V(t+4)=235+46.4*dcn(t)** (red). The abscissa shows the observation time in the Sun; the solar wind data are given with a shift of 4 days.

At the end of 2005, there was a relatively long period when no significant full halo frontsided CME were observed (DOY 250-365).

Fig. 10 illustrates the measured and calculated SW velocities for DOY 266–361 also with one lacuna. The correlation between the measured and calculated values is quite satisfactory. The correlation of ***dcn*** with the velocity at a shift of 4 days is fairly good amounting to 0.56.

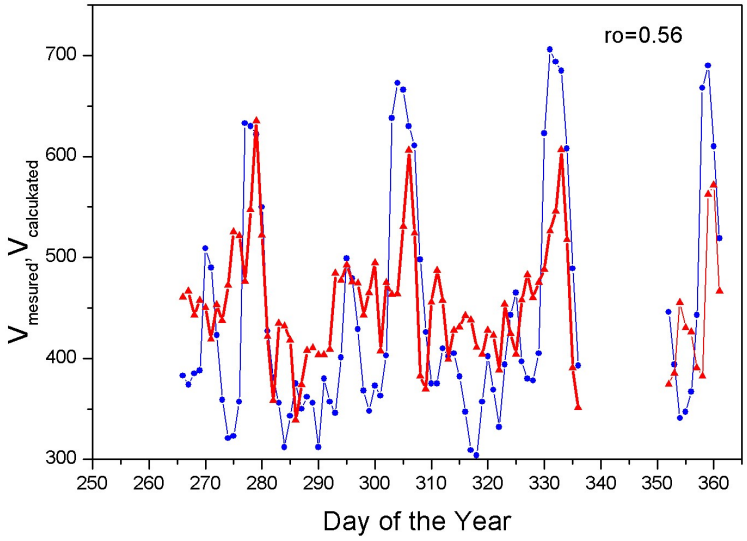

Fig. 10. Measured and calculated SW velocities for DOY 266–361

Note that we have assumed the standard transport time equal to 4 days, while, as seen from the figures and tables above, the real shift ranges from 3 to 5 days.

And finally, we have considered the period from November 21 to December 26, 2003, also free of CME events. This interval was also analyzed in (*Luo et al., 2008).* The correlation between the mean brightness and velocity at a 4-day shift coincides in both works and amounts to 0.89.

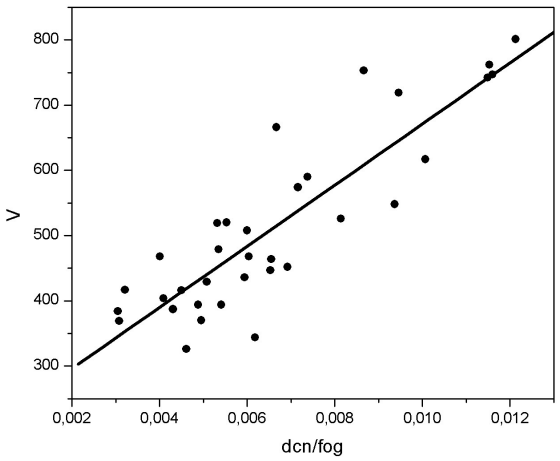

Fig. 11. Correlation between the mean deficit of ***dcn*** *and SW velocity for the period from November 21 to December 26, 2003.*

The scatter plot in Fig. 11 illustrates the correlation between the mean deficit of ***dcn*** and SW velocity for the period mentioned above. The abscissa gives the **dcn/fog** ratio over a time interval short enough not to affect the degradation. Here, the correlation coefficient is 0.89, which coincides with the value obtained by *Luo et al, (2008)* for the same period.

Fig. 12 shows the measured and calculated SW velocity over the time interval under discussion.

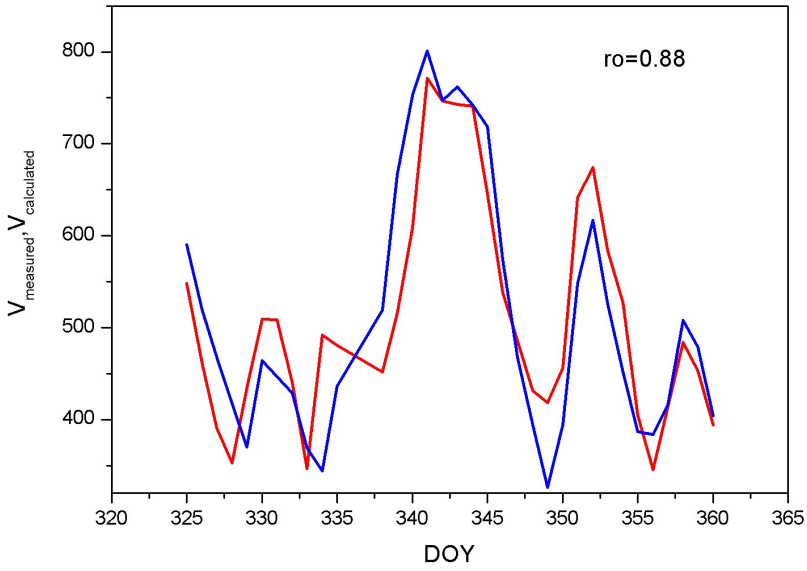

Fig. 12. Measured and calculated SW velocity for the time interval from November 21 to December 26, 2003.

Thus, calculation of the quiet solar wind velocity from the brightness deficit in coronal holes is fully justified for the periods when the disturbing effect of coronal mass ejections is absent.

An important thing to emphasize is that, regardless of the correlation coefficient, all events of the increase of velocity above 500 km/s recorded during the periods under discussion are well described by our calculated curves. The mean difference between the calculated and measured values is less than 50 km/s.

The presence of CME, however, changes the situation dramatically.

4.2. VIOLATION OF RELATIONSHIPS IN THE PRESENCE OF HALO FRONTSIDED CME

Daily indices have been calculated for the second half of 2005, when a number of halo frontsided CME were observed. Naturally, the CME events were found out to distort the statistics based on coronal holes. Fig. 13 illustrates the calculated and measured velocities for DOY 125-250 with one lacuna. In this case, the calculation equation was altered a little to have the form ***V(t+4)=200+50*dcn,*** which did not affect the main conclusions. As in the figures above, the abscissa shows the observation time in the Sun; the SW velocity data are given with a shift of 4 days.

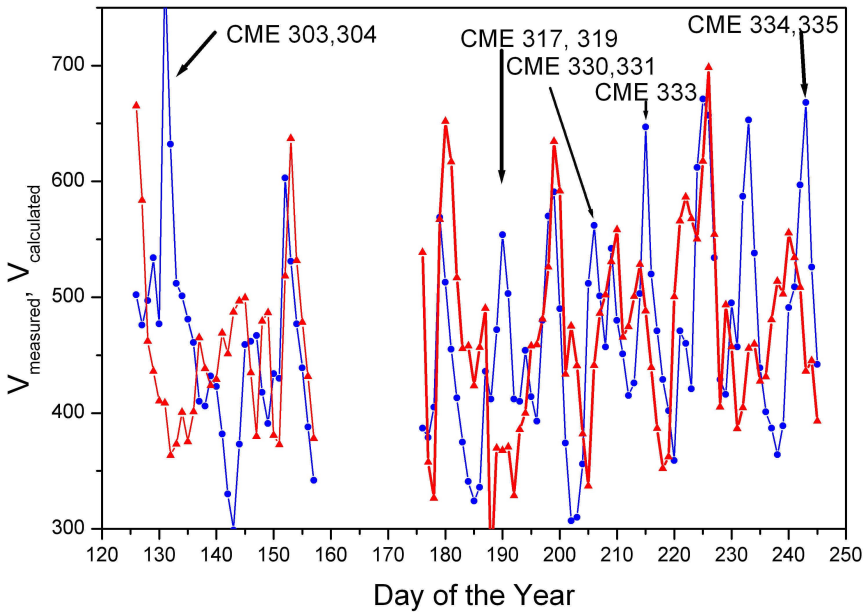

Fig. 13. Measured and calculated velocities for DOY 125-250.

As seen from the figure, the increase of SW velocity is not accompanied by the increase of ***dcn*** index in six cases. In five cases, the increase is definitely associated with CME events. The list of these CME with comments is given below. Data are taken from http://lasco-www.nrl.navy.mil/halocme.html

303 Full Halo CME on 2005/05/11, frontsided doy 131, associated with an M-class X-ray flare on NOAA AR 10758.

304 Full Halo CME on 2005/05/13, frontsided doy 133, associated with a LDE M-class X-ray event on NOAA AR 10759

317 Two frontsided events on 2005/07/07: II. M4.9 X-ray flare doy 188, associated with an M4.9 X-ray flare on NOAA AR 10786.

319 Full Halo Event on 2005/07/09, frontsided doy 190, associated with an M2.8 X-ray flare on NOAA AR 10786.

330 Asymmetric Full Halo Event on 2005/07/27 doy 208, determined as a strong limb event (barely backsided.

331 Asymmetric Full Halo Event on 2005/07/30, frontsided doy 211,associated with an X1.3 X-ray flare on NOAA AR 10792.

333 Frontsided event on 2005/08/05 doy 217, associated with the long duration C-class flare on AR 10792.

334 Complex Event on 2005/08/31 doy 242,

335 Faint Full Halo Event on 2005/08/31, frontsided doy 242, associated to a C-class X-ray event

The increase on DOY 233 (i.e., on August 22, 2005) remains unexplained. The catalogue http://lasco-www.nrl.navy.mil/halocme.html does not contain information of CME on that day. But according to the catalogue by Gopalswamy et al. (2008) *http://cdaw.gsfc.nasa.gov/CME_list*, CME events were recorded on August 22 and 23, though their source was close to the western limb, and it was not clear whether they were frontsided CME.

Thus, all reported increases of SW velocity not predicted by our calculations were determined entirely by CME.

Note also that our calculations do not describe well enough the cases of extremely low SW velocities, the cause of which still remains obscure. It may be the fact that the transport time at extremely low velocities is more than 4 days.

Conclusion

Thus, the hypothesis of direct correlation between the velocity of the quiet solar wind and CH contrast has been verified for all days in 2005 when observations in 284 A were available (the total of 345 days), 35 days in 2003, and 139 separate observations of coronal holes from 2002 to 2005, i.e., more than 500 measurements. The length of the time interval under consideration is about 1500 days in the declining phase of cycle 23. All coronal holes recorded in this period in the absence of coronal mass ejections have been analyzed. On the whole, it can be stated that the hypothesis is fully corroborated. With the transport time of 4 days, the correlation coefficient is occasionally as high as 0.89. All increases of velocity above 500 km/s recorded during the periods under discussion are well described by our calculated curves. The mean difference between the calculated and measured values is less than 50 km/s.

This allows the use of the method for direct prediction.

The contrast of coronal holes is rather small amounting, on the average, to 0.08 of the ambient regions and ranging from 0.04 to 0.013.

Acknowledgments

We are grateful to the SOHO team for the data available on the Internet site http://sohowww.nascom.nasa.gov/cgi-bin/summary_query_form, as well as to the authors of the sites Coronal hole history (since late October 2002) - http://www.dxlc.com/solar/coronal_holes.html and http://nsssdc.gsfc.nasa.gov/omniweb/. The calculations were partly fulfilled using the program by I.M. Livshits. We also thank A.V.Belov and I.M.Chertok for useful discussions. The work was supported by the Russian Foundation for Basic Research, project no. 08-02-00070.

References

Arge, C. N. and Pizzo, V. J.: 2000, *J. Geophys. Res.* **105**, 10465.

Arge C.N., D. Odstrcil, V.J. Pizzo and L.R. Mayer.: 2003, In Solar Wind Ten, edited by M. Velli, R. Bruno, and F. Malara, AIP Conf. PR0c. 2003. V.679. P.190.

Arge C.N., Luhmann, J.G., Odstrcil, D., Scrijver, C.J., and Li, Y.: 2004., J.Atmos.Sol.Terr.Phys. V.66.P.1295.

Badalyan, O. G. and. Obridko, V. N.: 2004, Astronomy Reports 48(8), 678-687.

Badalyan, O. G. and Obridko, V. N.: 2007, Solar Phys. **238**, Issue 2, .271, DOI 10.1007/s11207-006-0214-2 v 238, pp. 271-292
Belov A. V., Obridko V. N., and Shelting B. D.: 2006 Geomagn. Aeron. **46**, 430.
Bromage, B. J. I., Browning, P. K., and Clegg, J. R.:2001, Space Sci. Rev. **97**,13.
Chertok, I. M., Mogilevsky, E. I., Obridko, V. N., Shilova N. S., and Hudson, H. S.: 2001, Astrophys. J. **567**, 1225.
Cranmer, S.R.: 2002a, Yohkoh 10th Anniversary Meeting. Proceedings of the conference held September 17-20, 2001, at King Kamehameha's Kona Beach Hotel in Kailua-Kona, Hawaii, USA. Edited by P.C.H. Martens and D. Cauffman. Published by Elsevier Science on behalf of COSPAR in the COSPAR Colloquia Series, 2002., p.3
Cranmer, S.R.: 2002b, Space Sci. Rev., v. 101, Issue 3, p. 229-294
Cushman, G.W. and Rense, W.A.: 1976, Astrophys . J**. 207**, L61.
Gosling, J. T. and Pizzo, V. J.: 1999, Space sci. Rev. **89,** 21.
Gopalswamy, N., Yashiro, S., Michalek, G., Vourlidas, A., Freeland, S., and Howard, R. A..: 2008, THE SOHO/LASCO CME CATALOG,. http://www.iiap.res.in/events/ihy/school/gopalswamy_lecture.pdf
Kahler, S. W. and Hudson, H. S.: 2002, Astrophys. J. **574**, 467.
Luo, B., Zhong, Q., Liu, S., and Gong, J. : 2008, Solar Phys., 250, 159
McComas, D. J. and Elliot, H. A.: 2002, Geophys. Res. Lett. **29**,1314.
Nolte, J. T., Krieger, A. S., Timothy, A. F., Gold, R. E., Roelof, E. C., Vaiana, G., Lazarus, A. J., Sullivan, J. D., and McIntosh, P. S.: 1976, Solar Phys. **46**, 303.
Obridko V.N.: 1998, in ADVANCES IN SOLAR CONNECTION WITH INTERPLANETARY PHENOMENA, Proceedings of the third SOLTIP Symposium, Beijing, China, October 14-18, 1996, 41.
Obridko, V. N., Fomichev, V. V., Kharshiladze, A. F., Zhitnik, I., Slemzin, V., Wu, S. W., Ding, J., and Hathaway, D.: 2000, Astron. and Astrophys. Transactions, **18**, N.6, 819.
Obridko, V. N. and Shelting, B. D.: 1999, Solar Phys. **187,**185.
Obridko, V. N. and Shelting, B. D.: 2009, Astronomy Letters, V 35, №3, pp. 38.
Obridko, V. N., Shelting B. D., and Kharshiladze A. F.:2004, Astron. Vestn. **38** (3), 261
Obridko, V. N., Shelting B. D., and Kharshiladze A. F. 2006, Geomagn. Aeron. **46**, 294.
Orrall, F.Q., Rottman, G.J., and Klimchuk, J.A.: 1983, Ap. J. **266**, L65.
Robbins, S., Henney, C. J., and Harvey, J.W.: 2006, Solar Phys**. 233**,265.
Rottman, G.J., Orrall, F.Q., and Klimchuk, J.A.: 1982, Ap. J**. 260**, 326.
Veselovsky, I. S., Persiantsev, I. G., Ruasanov, A. Yu., and Shugai, Yu. S.:2006, Solar Syst. Res. **40**, 427.
Vrsnak, B., Temmer, M., and Veronig, A. M.: 2007a, Solar Phys. **240**, 315.
Vrsnak, B., Temmer, M., and Veronig, A. M.: 2007b, Solar Phys**. 240**, 331.
Wang, Y.-M. and Sheeley, N. R., Jr.: 1990, *Astrophys. J.* **355**, 726.
Wang, Y.-M. and Sheeley, N. R., Jr.: 1992, *Astrophys. J.* **392**, 310.
Withbroe, G.L., and Noyes, R.W.: 1977, In: Annual review of astronomy and astrophysics. Volume 15. (A78-16576 04-90) Palo Alto, Calif., Annual Reviews, Inc., 1977, p. 363
Zhang, J., Woch, J., Solanki, S. K., and von Steiger, R.: 2002, Geophys. Res. Lett**. 29**, 1236.
Zhang, J., Woch, J., Solanki, S. K., von Steiger, R., and Forsyth, R.: 2003, J. Geophys. Res. **108,** 1144.
Zhao, X. P., Hoeksema, J. T., and Scherrer, P. H.:1999, J. Geophys. Res. **104**, 9735.